(17) Kant, J. A., *J. Chem. Phys.*, **41**, 1872 (1964).
(18) Kelley, K. K., "Contributions to the Data on Theoretical Metallurgy; XIII. High Temperature Heat Content, Heat Capacity, and Entropy Data for the Elements and Inorganic Compounds," Bulletin 584, Bureau of Mines, Washington, D.C., 1960.
(19) Kellogg, H. H., *J. Chem. Eng. Data*, **14**, 41 (1969).
(20) Kieffer, L. J., Dunn, G. W., *Rev. Mod. Phys.*, **38**, 1 (1966).
(21) King, E. G., *J. Amer. Chem. Soc.*, **79**, 2399 (1957).
(22) Langmuir, I., Jones, H. A., MacKay, G. M. J., *Phys. Rev.*, **30**, 26 (1927).
(23) Langmuir, I., "The Collected Works of Irving Langmuir," Vol 9, p 3, Pergamon, New York, N.Y., 1916.
(24) Mallet, L., Rosen, B., *Bull. Soc. Roy. Sci., Liege*, **14**, 382 (1945).
(25) Mandel, John, "The Statistical Analysis of Experimental Data," Chap. 5, Interscience, New York, N.Y., 1964.
(26) Mandel, John, Paule, R. C., *Anal. Chem.*, **42**, 1194 (1970).
(27) Moore, C. E., *Nat. Bur. Stand.*, Circular No. 467, 1959.
(28) Morris, J. P., Zellars, G. R., Payne, S. L., Kipp, R. L., "Vapor Pressure of Liquid Iron and Liquid Nickel," U.S. Bureau of Mines, Report No. 5364, 1957.
(29) Nesmeyanov, An. N., Tik-Mang, Teh, *Dokl. Akad. Nauk SSSR*, **116**, 230 (1957).
(30) Nesmeyanov, An. N., Tik-Mang, Teh, *Izv. Akad. Nauk SSR, Otd. Tekh. Nauk* (1), 75 (1960).
(31) Nesmeyanov, An. N., "Vapor Pressure of the Elements," J. I. Carasso, Transl., p 396, InfoSearch, London, England, 1963.
(32) Oetvos, J. W., Stevenson, D. P., *J. Amer. Chem. Soc.*, **78**, 546 (1956).
(33) Paule, R. C., Mandel, John, "Analysis of Interlaboratory Measurements on the Vapor Pressures of Cadmium and Silver," NBS Spec. Publ. 260-21, Nat. Bur. Stand., Washington, D.C., 1971.
(34) Pauling, L., "Nature of the Chemical Bond," (a) p 62, (b) p 256, Cornell Univ. Press, Ithaca, N.Y., 1960.
(35) Rovner, L. H., Norman, J. H., *J. Chem. Phys.*, **52**, 2496 (1970).
(36) Rutner, Emile, Haury, G. L., "The Vapor Pressure and Heats of Vaporization of Nickel," Tech. Report AFML-TR-72-217, Air Force Materials Lab, Wright-Patterson AFB, Ohio, 1972.
(37) Stull, D. R., Sinke, G. C., "Thermodynamic Properties of the Elements," American Chemical Society, Washington, D.C., 1956.
(38) Trivedi, Hrishikesha, *Proc. Nat. Acad. Sci., India*, *4*, 27 (1935).
(39) Wang, K. L., Brody, M. D., Crawford, C. K., Air Force Materials Lab, Report AFML-TR-69-5, Jan. 1969.
(40) Weast, R. C., Ed., "Handbook of Chemistry and Physics," 47th ed., Chemical Rubber Co., Cleveland, Ohio, 1966.
(41) Wickes, C. E., Block, F. E., "Thermodynamic Properties of 65 Elements, Their Oxides, Halides, Carbides, and Nitrides," Bulletin 605, Bureau of Mines, Washington, D.C., 1963.
(42) Yamashito, Jiro, Masa, Kojima, *J. Phys. Soc., Japan*, *7* (3), 261 (1952).

Received for review May 14, 1973. Accepted September 27, 1973.

Liquid and Vapor Densities of Aluminum Bromide

David S. Olson, Fred C. Kibler, Jr., David W. Seegmiller, Armand A. Fannin, Jr., and Lowell A. King[1]
Frank J. Seiler Research Laboratory (Air Force Systems Command) and Department of Chemistry, United States Air Force Academy, Colo. 80840

The orthobaric liquid and vapor densities of aluminum bromide were measured from 92° to 319°C. The method simultaneously yielded the liquid and vapor densities for each (arbitrary) experimental temperature. The experimental precision was ±0.0025 g/cm^3, which corresponds to 0.1% of the liquid densities, and ranged from 6 to 100% of the vapor densities over the temperature range covered. A single empirical equation was derived which was symmetrical about the rectilinear diameter and which represented both liquid and vapor densities.

As part of a program for the investigation of certain low-melting, molten salt electrolytes for high energy density batteries, we needed to know the densities of aluminum bromide liquid and vapor. Many of the physical properties of aluminum bromide have been collected in a review by Boston (*2*). Biltz and Voight (*1*) earlier had measured a few liquid densities from 100° to 265°C, Zhuravlev (*10*) measured liquid densities from 170° to 450°C, and Johnson et al. (*4*) determined liquid and vapor densities in the temperature ranges 101–490°C and 270–488°C, respectively. We were interested primarily in the densities near the melting point, which was reported to be 97.5°C (*9*).

Experimental

Aluminum bromide was synthesized by dropping Mallinckrodt analytical reagent Br_2 onto J. T. Baker purified granular aluminum contained in a flask in which a slight positive pressure of dry Ar was maintained. After the synthesis was complete, $AlBr_3$ was distilled out of the reaction flask into a clean container. The distillate crystals were transferred (inside a glove box) to an ampul which was then evacuated and sealed, and a further purification carried out by growing crystals from the vapor phase. This latter process was done in a manner analogous to the method we formerly used for $AlCl_3$ (*8*).

Orthobaric liquid and vapor densities were simultaneously determined from 363 measurements made substantially as we reported earlier for our work with aluminum chloride (*5*, *7*). Thirteen sealed borosilicate glass dilatometric tubes were used. These each consisted of two bulbs connected by a calibrated, graduated capillary. The tubes were held vertically, such that liquid $AlBr_3$ filled the lower bulb and extended into the graduated capillary. The upper part of the capillary and the upper bulb contained $AlBr_3$ vapor.

The filled bulbs were immersed in a molten salt bath, and at each different temperature the distance from the bottom of the $AlBr_3$ meniscus to an arrow etched on the capillary was measured with the aid of a cathetometer. From this measurement and the tube calibration data, the liquid volume was calculated.

The dilatometric tubes were identical in general size and design to those described in ref. *5*. They were calibrated in the same manner employed for tubes *A*, *B*, *C*, and *D* of that report. Meniscus corrections and thermal expansion corrections, the molten salt bath, and the bath temperature control were also as described therin. Bath temperature was determined by measuring the resistance of a 4-wire platinum resistance element (Electric Thermometers Trinity, Inc., Bridgeport, Conn. 06604) (100 Ω nominal) calibrated against the platinum Air Force Reference Standard Thermometer which we used earlier (*7*).

Tube calibration data are given in Tables I and II. The distances from $AlBr_3$ menisci to the arrows etched on the capillaries are shown in Table III. Without using unduly large capillaries (or small bulbs), it was not possible for a single tube to span the entire temperature range of interest. We divided the 13 tubes into five groups covering

[1] To whom correspondence should be addressed.

overlapping temperature ranges. The data in Table III were not all taken in the order listed; measurements were made with both ascending and descending temperature.

Results

At a given temperature, liquid and vapor densities are related to the tube parameters and mass of $AlBr_3$ by the set of equations

$$DV_i + d(T_i - V_i) - m_i = 0 \quad (1)$$

According to the law of the rectilinear diameter, the mean of the orthobaric densities of a substance is a linear function of temperature; that is,

$$\rho_m = \frac{D + d}{2} = \rho_c + a_0\tau \quad (2)$$

where

$$\tau = t_c - t;\ t_c = 490°C \ (4)$$

In other words, the liquid and saturated vapor densities of a substance should describe a symmetrical function about the rectilinear diameter. We assumed the liquid and vapor densities of $AlBr_3$ were related to temperature by the equation

$$\tau + a_2Q^2 + a_3Q^3 = 0 \quad (3)$$

where

$$Q = D - \rho_m = \rho_m - d \quad (4)$$

From Equations 1, 2, and 4, it is possible to derive the equation

$$Q_{tube} = \frac{\rho_m - \rho}{1 - 2\phi} \quad (5)$$

Table I. Calibration of Density Tubes: τ and m

Tube identifier	Total enclosed vol, cm^3 (25°C)	Mass of $AlBr_3$ in tube, g
A1	79.17[a]	27.797[b]
B1	108.47	34.943
C1	55.30	28.273
D1	31.28	25.701
E1	26.11	29.967
A2	81.64	25.510
D2	36.54	24.329
F2	56.96	22.835
A3	80.31	24.141
C3	56.14	25.146
D3	31.65	22.828
E3	26.72	26.747
G3	84.56	29.50

[a]Estimated uncertainty in $\tau = \pm 0.05\ cm^3$. [b]Estimated uncertainty in $m = \pm 0.003$ gram.

Table II. Calibration of Density Tubes: Fixed Parameters

Letter of tube identifier	Vol to arrow, cm^3 (25°C)	Vol of capillary, cm^3/cm (25°C)
A	10.478 ± 0.001	0.0653 ± 0.0006
B	13.8127 ± 0.0006	0.0610 ± 0.0004
C	10.898 ± 0.003	0.066 ± 0.002
D	10.018 ± 0.002	0.0662 ± 0.0009
E	11.7297 ± 0.0007	0.0665 ± 0.0004
F	9.468 ± 0.001	0.0669 ± 0.0004
G	12.798 ± 0.004	0.066 ± 0.001

Table III. Experimental Measurements

Height of meniscus — height of etched arrow, cm[a]

Temp, °C	Tube *A1*	Tube *B1*	Tube
91.89[b]	−1.230		
96.99	−0.515		
102.21	0.175		
107.32	0.895		
112.57	1.580		
117.78	2.300		
122.98	3.045		
128.19	3.745		
133.39	4.495		
138.63	5.185	−3.595	
143.93		−2.590	
149.24		−1.380	
154.53		−0.340	
157.49		0.110	
158.49		0.200	
159.82		0.535	
160.04		0.470	
161.04		0.700	
162.32		0.875	
165.04		1.360	
165.18		1.520	
166.17		1.555	
168.97		2.105	
169.99		2.395	
170.63		2.550	
171.31		2.620	
172.79		2.865	
175.00		3.260	
175.99		3.475	
179.64		4.155	
179.99		3.530	
180.13		4.280	
181.31		3.855	
182.66		4.080	
182.68		4.575	
184.07		4.460	
185.19		5.140	
185.34		4.715	
186.72		5.335	
186.80		5.050	
188.11		5.365	
	C1	*D1*	*E1*
93.12	−4.485		
98.28	−4.080	−4.695	
103.40	−3.170	−4.015	
106.04	−2.715	−3.665	−5.285
108.67	−2.465	−4.095	−4.780
111.27	−2.065	−3.690	−4.315
113.87	−1.580	−3.230	−3.930
116.45	−1.285	−2.740	−3.485
120.18	−0.630	−1.820	−2.900
121.81	−0.500	−1.615	−2.665
124.40		−1.270	−2.220
126.96	0.285	−0.910	−1.850
129.61	0.720	−0.550	−1.420
132.15	1.055	−0.115	−0.995
134.78	1.435	0.255	−0.580
136.18	1.625	0.435	−0.375
137.47	1.810	0.620	−0.185
138.84	1.990	0.795	0.005
140.16	2.215	0.980	0.260
141.45	2.395	1.170	0.480
142.80	2.610	1.370	0.725
144.09	2.775	1.555	0.905

(Continued)

Table III. Continued

Height of meniscus—height of etched arrow, cm[a]

Temp, °C	Tube	Tube	Tube
	C1	*D1*	*E1*
145.46	2.990	1.770	1.115
146.71	3.195	1.955	1.335
148.08	3.350	2.120	1.545
149.36	3.580	2.325	1.795
150.28	3.675	2.450	1.925
152.96	4.145	2.855	2.370
153.92	4.520		2.600
155.01	4.545	2.870	2.525
155.14	4.725	3.130	2.830
155.72	4.810	3.210	2.925
155.78	4.520	3.130	2.805
156.92	4.990	3.370	3.130
157.61	5.110	3.475	3.235
158.28		3.575	3.370
158.28		3.580	3.360
158.57	4.900	3.535	3.295
158.78		3.650	3.455
159.45		3.740	3.570
159.85		3.770	3.640
161.15		3.920	3.755
163.20		4.265	4.195
163.90		4.340	4.200
	A2	*F2*	*D2*
165.77	−4.225	−5.150	−3.930
171.33	−3.540	−4.465	−3.210
175.94	−2.910	−3.810	−2.540
176.10	−2.845	−3.995	−2.535
178.50	−2.640	−3.845	−2.395
182.22	−2.150	−3.375	−1.690
182.33	−1.905	−3.150	−1.635
183.73	−1.780	−2.975	−1.455
185.38	−1.555	−2.780	−1.225
188.26	−1.395	−2.675	−0.860
192.26	−0.740	−1.980	−0.275
195.67	−0.440	−1.825	0.175
197.34	−0.375	−1.670	0.190
200.66	0.170	−1.280	0.860
203.32	0.475	−0.975	1.230
205.57	0.725	−0.730	1.540
208.19	0.995	−0.455	1.900
209.36	1.075	−0.315	1.895
210.78	1.305	−0.165	2.260
213.26	1.590	0.110	2.590
215.64	1.915	0.460	2.905
215.74	1.860	0.380	2.940
218.23	2.095	0.635	3.245
220.69	2.355	0.940	3.640
221.08	2.485	1.205	3.505
223.13	2.620	1.185	3.980
225.66	2.885	1.470	4.310
228.02	3.115	1.825	4.640
229.24	3.085	2.360	4.785
230.08	3.310	2.075	4.960
230.38	3.515	2.375	4.965
231.10	3.540	2.730	5.050
231.12	3.540	2.665	5.100
	A3	*D3*	*E3*
224.99	−5.435		
229.53	−5.195	−4.665	−4.865
229.90	−5.180		
230.55	−5.110	−4.505	−4.725
232.39	−5.010	−4.220	−4.355
233.16	−5.200		

Temp, °C	Tube	Tube	Tube
	A3	*D3*	*E3*
234.70	−4.845	−3.915	−3.960
236.53	−4.080		
237.70	−4.815		
239.73	−4.350	−3.145	−3.035
240.31	−3.795		
243.81	−4.125	−2.690	−2.385
245.24	−3.630		
247.10	−3.830		
248.24	−3.805		
249.06	−3.805		
249.07	−3.805		
249.30	−3.750	−1.905	−1.430
250.17	−3.100		
253.34	−3.565	−1.350	−0.730
254.62	−3.575		
255.13	−2.780		
258.40	−3.080	−0.665	0.160
259.68	−2.750		
264.48	−2.740	0.150	1.230
264.54	−2.775		
264.87	−2.390		
269.48	−2.905		
269.59	−2.305		
269.59	−2.900		
269.59	−2.920		
269.65	−2.685		
269.66	−2.460		
269.67	−2.725		
269.69	−2.630		
269.73	−2.555		
269.86	−2.200		
273.15	−2.395	1.330	2.815
274.77	−2.090		
279.71	−1.950		
282.82	−2.225	2.625	4.595
284.25	−2.080		
288.75	−2.525		
289.00	−1.890		
293.63	−2.055		
294.28	−2.260	4.170	
305.68	−2.620		
317.64	−3.525		
329.03	−4.405		
	C3	*G3*	
244.19	−2.475	−5.395	
249.11	−1.740	−4.480	
254.73	−1.125	−3.670	
257.80	−0.855	−3.660	
261.44	−0.380	−3.155	
264.81	−0.100	−2.990	
268.44	0.375	−2.550	
277.28	1.335	−1.855	
282.04	1.640	−1.845	
287.28	1.965	−1.530	
292.04	2.355	−1.345	
296.63	2.680	−1.170	
301.71	2.975	−1.015	
308.90	3.420	−0.390	
318.75	3.710	0.150	

[a]Total estimated uncertainty in distance from meniscus to arrow = ±0.005 cm. [b]Estimated uncertainty in temperature = ±0.05°C.

where

$$\rho = \frac{m}{T} \text{ and } \phi = \frac{V}{T}$$

Equation 5 is a function of the cathetometer measurements and the tube calibration data. The value of Q_{tube} can be calculated for each tube at each temperature from the adjustable constants a_0 and ρ_c and the data from Tables I–III.

Equation 3 is cubic in Q. For the particular values of a_2 and a_3 which best represent our data, Equation 3 has two imaginary roots and one real root. The real root is

$$Q_{eqn} = \{-(A + B\tau) + [(2A + B\tau)B\tau]^{1/2}\}^{1/3} + \{-(A + B\tau) - [(2A + B\tau)B\tau]^{1/2}\}^{1/3} - A^{1/3} \quad (6)$$

where

$$A = \left(\frac{a_2}{3a_3}\right)^3 \text{ and } B = \frac{1}{2a_3}$$

Equation 6 is a function of the adjustable constants a_2 and a_3 and is not directly dependent on the data of Tables I–III.

A least-squares fit was made of the function

$$z_i = Q_{eqn,i} - Q_{tube,i} \quad (7)$$

for the values of adjustable constants a_0, a_2, a_3, and ρ_c which minimized the sum

$$\sum_{i=1}^{n} (z_i)^2$$

All the experimental points represented in Table III were given equal weights in the least-squares calculations. The standard deviation is in Q and is defined by

$$\sigma = \left[\frac{1}{n-4}\sum_{i=1}^{n}(z_i)^2\right]^{1/2} \quad (8)$$

The results of the least-squares fit are given in Table IV. The estimated errors in each of the parameters are the changes in that parameter which will change Q by one standard deviation, σ.

Table IV. Equations for $AlBr_3$ Density[a]

For liquid: 92–319°C; vapor: 180–319°C

$$D \text{ or } d\ (g/cm^3) = \rho_c + a_0\tau \pm [\{-(A + B\tau) + [(2A + B\tau)B\tau]^{1/2}\}^{1/3} + \{-(A + B\tau) - [(2A + B\tau)B\tau]^{1/2}\}^{1/3} - A^{1/3}] \quad (10)$$

$$A = \left(\frac{a_2}{3a_3}\right)^3;\ B = \frac{1}{2a_3}$$

$a_0 = (1.176 \pm 0.001) \times 10^{-3}$
$a_2 = 55 \pm 2$
$a_3 = -214 \pm 1$
$\rho_c = 0.8622 \pm 0.0003$ g/cm³
$\sigma = \pm 0.0025$ g/cm³

For vapor: 97.5–180°C

$$d = b_0 + b_1\tau + b_2\tau^2 + b_3\tau^3 \quad (11)$$

$b_0 = -2.5509 \times 10^{-2}$
$b_1 = 3.3803 \times 10^{-4}$
$b_2 = -1.2122 \times 10^{-6}$
$b_3 = 1.3176 \times 10^{-9}$

[a] In Equation 10, + term yields D and − term yields d.

Equations 3 or 10 can be solved to yield vapor density over the entire experimental temperature region; however, the estimated error becomes larger than the actual $AlBr_3$ vapor density at low temperatures. One result of this is that the equation predicts vapor densities which *increase* as the temperature falls below approximately 165°C. The calculated densities all fall within the range of experimental scatter down to the lowest temperature reached, 92°C; nevertheless, this clearly is an unsatisfactory situation. Several other functions were fit instead of Equation 3, including the form we used with $AlCl_3$ (*7*) and the modified Guggenheim equation previously used with $AlBr_3$ (*4*). Without exception, all of these equations even more poorly represented the vapor density–temperature behavior at low temperatures.

Accordingly, we decided to represent the low-temperature vapor densities by the polynomial in τ

$$d = \sum b_i\tau^i \quad (9)$$

The selected polynomial was to be monotonic over its entire range of use. In addition, the following four constraints were applied: The density and slope calculated from Equation 9 were required to match the density and slope calculated from Equation 10 at their point of intersection. Also, the density and slope calculated from Equation 9 were required to match the density and slope at the melting point, 97.5°C, as calculated from the ideal gas law and the vapor-pressure data of Fischer et al. (*3*). (These values are $d_{\text{melting point}} = 9.46 \times 10^{-5}$ g/cm³ and $(\partial d/\partial t)_{\text{melting point}} = 4.59 \times 10^{-6}$ g/cm³ deg).

The lowest convenient intersection temperature (to the nearest even number of degrees) which yielded a monotonic function from the melting point to the intersection temperature (indeed, to the critical point) was 180°C. Since there were four specific constraints, we chose a polynomial having four terms, thereby specifying each of the parameters, b_i. The resulting equation is given in Table IV as Equation 11.

Discussion

Together, Equations 10 and 11 yield the liquid densities with an estimated error of ±0.1%, which compares well with previous results for $AlBr_3$ (*4*) and with our results for $AlCl_3$ (*5, 7*). The vapor densities have an estimated error of ±6% at the highest temperatures. This is about the same error as reported by Johnson et al. (*4*) at the same temperature region, which was the minimum temperature reached in their vapor density measurements. The error in vapor density increases, of course, as temperature falls.

If the experimental liquid and vapor densities were to be plotted on Figure 1, which illustrates the entire coexistence curve for $AlBr_3$, virtually all 726 points would fall within the thickness of the line (which is 2 σ wide) used to portray Equations 10 and 11.

The critical temperature has been reported variously as 490° (*4*), 495° (*10*), and 499°C (*6*). We used 490°C in our equations. Critical densities of 0.8605 ± 0.0023 g/cm³ (*4*) and 0.8875 g/cm³ (*10*) have been reported. Even though our highest temperature investigated was approximately 170° below the critical point, we found a least-squares fit ρ_c which lay within the estimated error limits of Johnson et al. (*4*). Their value of a_0, 1.1758×10^{-3}, also agrees with the present value of $(1.176 \pm 0.001) \times 10^{-3}$. It should not be surprising, then, that Equations 10 and 11 can be used to find liquid and vapor densities over the entire liquid region up to the critical

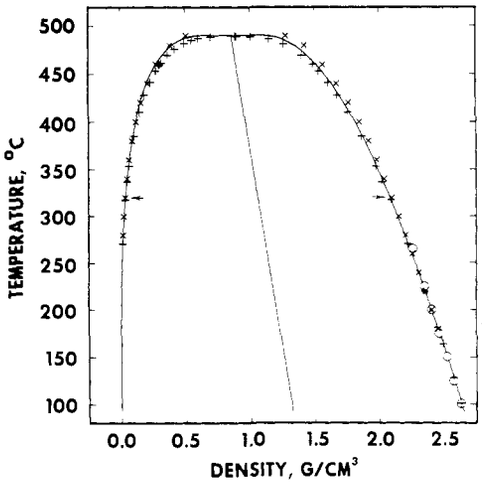

Figure 1. Coexistence curve for aluminum bromide
——, Calculated from Equations 10 and 11; O, Biltz and Voight (*1*); ×, Zhuravlev (*10*); +, Johnson et al. (*4*). Arrows indicate highest experimental temperature reached in present work

temperature. Indeed, the experimental points observed by Johnson et al. lie slightly below Equation 10 at temperatures above our highest temperature. Similarly, Zhuravlev's liquid density data lie slightly above our Equation 10, also above our highest temperature. These data are shown in Figure 1.

Safety

The same precautions should be taken as were reported previously (*5*) for the containment of liquids above their normal boiling points in glass vessels.

Nomenclature

a_i = empirical coefficients
A = constant, a function of a_2 and a_3
b_i = empirical coefficients
B = constant, a function of a_3
d = density of $AlBr_3$ vapor
D = density of $AlBr_3$ liquid
m_i = mass of $AlBr_3$ in ith tube
n = number of individual experimental measurements
Q = positive difference between rectilinear diameter and d or D
T_i = total enclosed volume in ith tube
t = temperature in degrees centigrade
t_c = critical temperature
V_i = liquid $AlBr_3$ volume in ith tube
z_i = residual; function to be treated by least-squares fitting
ρ = overall tube average density; i.e., m/T
ρ_c = density at critical temperature
ρ_m = rectilinear diameter; i.e., $(d + D)/2$
σ = standard deviation in Q
τ = distance from critical temperature, i.e., $t_c - t$
ϕ = fraction of total tube volume occupied by liquid; i.e., V/T

Literature Cited

(1) Biltz, W., Voight, A., *Z. Anorg. Allgem. Chem.*, **126,** 39 (1923).
(2) Boston, C. R., in "Advances in Molten Salt Chemistry," Chap. 3, J. Braunstein, G. Mamantov, and G. P. Smith, Eds., Plenum Press, New York, N.Y., 1971.
(3) Fischer, W., Rahlfs, O., Benze, B., *Z. Anorg. Allgem. Chem.*, **205,** 1 (1932).
(4) Johnson, J. W., Silva, W. J., Cubicciotti, D., *J. Phys. Chem.*, **72,** 1664 (1968).
(5) King, L. A., Seegmiller, D. W., *J. Chem. Eng. Data*, **16,** 23 (1971).
(6) Rotinjanz, L., Suchodski, W., *Z. Phys. Chem.*, **87,** 635 (1914).
(7) Seegmiller, D. W., Fannin, Jr., A. A., Olson, D. S., King, L. A., *J. Chem. Eng. Data*, **17,** 295 (1972).
(8) Seegmiller, D. W., Rhodes, G. W., King, L. A., *Inorg. Nucl. Chem. Lett.*, **6,** 885 (1970).
(9) "Selected Values of Chemical Thermodynamic Properties," Nat. Bur. Stand. Circular 500, p 731, 1952.
(10) Zhuravlev, D. I., *Zh. Fiz. Khim.*, **10,** 325 (1937).

Received for review May 29, 1973. Accepted September 19, 1973.

X-Ray Powder Data and Unit Cell Parameters of $MgCl_2 \cdot 6H_2O$

Charles A. Sorrell[1] **and Roy R. Ramey**
Department of Ceramic Engineering, University of Missouri, Rolla, Mo. 65401

Detailed X-ray powder data for $MgCl_2 \cdot 6H_2O$ were obtained by diffractometry by use of CuK_α radiation at 22°C. The data were indexed on a bimolecular monoclinic unit cell, space group C2/m, with a = 9.858 ± 0.001 Å; b = 7.107 ± 0.001 Å; c = 6.069 ± 0.001 Å; β = 93° 47′ ± 10′. Calculated density was 1.591 g/cm³, compared with a measured density of 1.593 ± 0.003 g/cm³.

The structure of magnesium chloride hexahydrate, $MgCl_2 \cdot 6H_2O$, was determined by Andress and Gundermann (*1*), who reported a bimolecular unit cell, space group C2/m, with a = 9.90 ± 0.03 Å; b = 7.15 ± 0.03 Å; c = 6.10 ± 0.03 Å; β = 94° ± 20′. The only available X-ray powder data appeared in the original Hanawalt et al. compilation (*3*) and was subsequently included in the "Powder Diffraction File" (*5*). Comparison of the structure factors calculated by Andress and Gundermann with the powder data indexed by J. V. Smith indicates the incomplete nature of the powder data. This, coupled with the relatively low precision of the reported unit cell parameter measurements, prompted acquisition of the data reported in this work.

[1] To whom correspondence should be addressed.

X-Ray Procedures

Powder data were acquired at 22°C by conventional methods by use of a General Electric XRD-700 recording diffractometer with CuK_α radiation generated at 50 kVp and 20 Ma. Flat recessed sample holders machined from Lucite were used. Samples containing approximately 20% high-purity rock crystal quartz as an internal standard were scanned from 2° to 60° 2 θ at a rate of 0.2° per min, which permitted measurement of 2 θ values to the nearest 0.01°. Samples containing no internal standard were then scanned, following alignment on the (020) line of the chloride, to provide complete interplanar spacing and intensity data.